

Morphological Analysis on the Coherence of kHz QPOs

J. Wang • H. K. Chang • C. M. Zhang •
D. H. Wang¹ • L. Chen • J. L. Qu • L. M. Song

Abstract We take the recently published data of twin kHz quasi-period oscillations (QPOs) in neutron star (NS) low-mass X-ray binaries (LMXBs) as the samples, and investigate the morphology of the samples, which focuses on the quality factor, peak frequency of kHz QPOs, and try to infer their physical mechanism. We notice that: (1) The quality factors of upper kHz QPOs are low ($2 \sim 20$ in general) and increase with the kHz QPO peak frequencies for both Z and Atoll sources. (2) The distribution of quality factor versus frequency for the lower kHz QPOs are quite different between Z and Atoll sources. For most Z source samples, the quality factors of lower kHz QPOs are low (usually lower than 15) and rise steadily with the peak frequencies except for Sco X-1, which drop abruptly at the frequency of about 750 Hz. While for most Atoll sources, the quality factors of lower kHz QPOs are very high (from 2 to 200) and usually have a rising part, a maximum and an abrupt drop. (3) There are three Atoll sources (4U 1728-34, 4U 1636-53 and 4U 1608-52) of displaying very high quality factors for lower kHz QPOs. These three

sources have been detected with the spin frequencies and sidebands, in which the source with higher spin frequency presents higher quality factor of lower kHz QPOs and lower difference between sideband frequency and lower kHz QPO frequency.

Keywords accretion: accretion disks–stars:neutron–binaries: close–X-rays: stars–pulsar

1 Introduction

The kilohertz quasi-periodic oscillations in neutron star X-ray binaries were discovered just two months after the launch of Rossi X-ray Timing Explorer (RXTE) in Sco X-1 (van der Klis et al. 1996a,b,c) and 4U 1728-34 (Strohmayer et al. 1996a,b,c). The former is a bright Z source, while the latter is an Atoll source. In general, Z sources produce the Z-shaped paths in CCDs or hardness-intensity diagram (HID) on timescales of a few hours to days, with three branches, from hard to soft: horizontal branch (HB), normal branch (NB), and flaring branch (FB). Z sources are objects with high luminosity ($0.5 - 1.5L_{Edd}$) (van der Klis 2006) and mildly high magnetic field (Miller et al. 1998; Campana 2000; Zhang 2007). The Atoll sources, with low luminosity ($\sim 0.001 - 0.2L_{Edd}$) (van der Klis 2006) and inferred weaker magnetic field (Miller et al. 1998; Campana 2000; Zhang 2007), show a hard, low-luminosity, fuzzy island state (IS) and a soft, high-luminosity "banana" shaped structure on a timescale of weeks (Hasinger et al. 1989; Hasinger 1990; van der Klis 2000, 2006). They trace a U-shaped or a C-shaped track as the sources spectrum evolves between the island and the banana (Gladstone et al. 2007).

These kHz QPOs in LMXBs are peaks with some width in their power density spectra (PDS), and their profiles can be described by the Lorentzian Function

J. Wang

H. K. Chang

Institute of Astronomy, National Tsing Hua University, Hsinchu, 30013, Taiwan

C. M. Zhang

National Astronomical Observatories, Chinese Academy of Sciences, Beijing, 100012, China

D. H. Wang

L. Chen

Astronomy Department, Beijing Normal University, Beijing, 100875, China

J. L. Qu

L. M. Song

Institute of High Energy Physics, Chinese Academy of Sciences, Beijing, 100049, China

¹National Astronomical Observatories, Chinese Academy of Sciences, Beijing, 100012, China

$P_\nu \propto A_0 w / [(\nu - \nu_0)^2 + (w/2)^2]$ (van der Klis 2000, 2006). Here, ν_0 is the peak frequency (or centroid frequency), w is the full width at half-maximum (FWHM), and A_0 is the amplitude of this signal. The ratio of these two quantities is the quality factor, i.e., $Q \equiv \frac{\nu_0}{w}$. Therefore, the kHz QPOs can be characterized by three characteristic quantities, i.e., ν_0 , quality factor (Q) and the fractional root-mean-squared (rms, which represents a measure of the signal strength and is proportional to the square root of the peak power contribution to the PDS). The quality factor characterizes the coherence of a QPO signal, and its value is related to the lifetime of the signal.

Most kHz QPO signals usually occur in twins. The centroid frequencies (or peak frequency, i.e. upper ν_2 and lower ν_1 frequency) changes with accretion rate. Each peak has a corresponding quality factor (i.e. upper Q_2 and lower Q_1). In the past few years, many works have been dedicated to the investigation for quality factor as a function of peak frequency of kHz QPOs (Barret et al. 2005a,b,c, 2006, 2007, 2008; Boutelier et al. 2009, 2010). Using RXTE data, (Barret et al. 2005a) studied 4U 1608-52 and revealed a positive correlation between ν_1 and Q_1 , up to a maximum of about $Q \sim 200$. Motivated by this idea, (Barret et al. 2005b, 2006) studied, in a systematic way, the QPO properties of 4U 1636-53 and the dependency of Q on ν . It is shown that Q_1 and Q_2 of 4U 1636-53 follow different tracks in a $Q-\nu$ plot, i.e. Q_1 increases with ν_1 up to 850Hz ($Q \sim 200$) and drops precipitously to the highest detected frequencies $\sim 920\text{Hz}$ ($Q \sim 50$), while Q_2 increases steadily all the way to the highest detectable QPO frequency. Moreover, Q_1 is higher than Q_2 (Barret et al. 2005b,c, 2006). The $Q-\nu$ distribution in the sources 4U 1735-44, 4U 1728-34 have the similar trend as 4U 1636-53 (Barret et al. 2006; Boutelier et al. 2009; Mendez 2006; Torok 2009). Besides, Mendez (2006) studied the relations between maximum amplitude and coherence of kHz QPOs for a dozen of NS LMXBs.

Although most attentions for the coherence of kHz QPOs have been focussed on the individual source, there are no work to perform contrastive investigation for the properties between different types of sources, e.g. Atoll and Z sources. Triggered by this background, in this paper, we study the recently published data of Q for twelve sources in terms of Atoll and Z types, i.e. seven Atoll sources (4U 1608-52, 4U 1636-53, 4U 1728-34, 4U 0614+09, Aql X-1, 4U 1820-30 and 4U 1735-44) and five Z sources (Sco X-1, Cyg X-2, GX 17+2, GX 5-1 and GX 340+0). We benefit from the existing studies and use the published data from the collection by (Mendez 2006). Besides, we also consider

the source XTE J1701-462, a peculiar source exhibiting typical Z behaviors in CCDs (Remillard & Lin 2006; Homan et al. 2006a,b, 2007) and evolving into an Atoll source at the end of its outburst (Homan et al. 2010). In section 2, we make a contrastive investigation for the quality factor as a function of kHz QPO peak frequency. The implications are discussed in section 3. Section 4 contains the summary.

2 Contrastive Analysis for the Coherence of kHz QPOs

In this section, we study the recently published data of quality factor as a function of peak frequency for seven Atoll and five Z sources, in order to find out the differences between Z and Atoll sources. At first, we put all the sources together and study the relations for $Q_1-\nu_1$ and $Q_2-\nu_2$. Secondly, we investigate their distinctive properties for Z and Atoll sources, respectively. All the data are obtained by Proportional Counting Array (PCA) on board the RXTE (see Méndez 2006 and references therein for the data selection). For the data, no filtering on the raw data is performed, i.e. all photons are used and only time intervals containing X-ray bursts are removed (Barret et al. 2005a,b,c, 2006, 2007).

2.1 The $Q-\nu$ Relations for Upper and Lower kHz QPOs

We put the twelve sources together and investigate the evolution of Q as a function of ν (see Fig. 1). From Fig. 1, we find that the values of Q_2 (in general, $Q_2 \sim 2-20$) are lower than those of Q_1 (up to 200) as a whole. The Q changes with ν very differently for upper and lower kHz QPOs, and the ranges of Q are also different.

For the upper kHz QPOs (see the left panel of Fig. 1), most data points of Q_2 locate in the range with low values, i.e. $Q_2 \sim 2-20$ and $\nu_2 \sim 450-1200\text{Hz}$. It can be seen that most sources follow the steadily rising track in the $Q_2-\nu_2$ plot. At the frequency of $\nu_2 \sim 1050\text{Hz}$, a transition presents for 4U 1728-34, i.e. Q_2 begins to drop with ν_2 . The Q_2 of XTE 1701-462 in Z phase present very large errors, clustering in a very narrow range of frequency.

As far as the profiles of lower kHz QPOs, It displays two different trajectories in the $Q_1-\nu_1$ plot (see the right panel of Fig. 1). The data points of Z sources follow the steadily rising tendency with low values of Q_1 ($Q_1 \sim 2-20$), and ν_1 covers a wide range of frequency ($\nu_1 \sim 150-825\text{Hz}$). However, most Q_1 for Atoll sources increase with ν_1 to a maximum and abruptly drop. The Q_1 can be very high and vary from 2 to 200.

The centroid frequencies for these sources cover a relatively narrow range $\sim 550 - 950$ Hz. Moreover, despite of the similar tendency, different sources show their own "substructures" in different regions in $Q_1 - \nu_1$ diagram, which we will discuss in detail in the following.

On the whole, the Q -factors of lower kHz QPOs for Atoll sources are about 10 times higher than that for Z sources for the same frequency.

2.2 The $Q - \nu$ Correlations for Z Sources

Two plots in Fig. 2 present the regular and steady tendency, formed by five Z sources and the Z phase of XTE 1701-462. It can be found that the $Q - \nu$ tracks of Z sources are similar between upper and lower kHz QPOs. For a close inspection, we find that different sources lie in different regions in the $Q - \nu$ plots, and it can be divided into two regions by the range of frequency for both upper and lower kHz QPOs. One contains GX 5-1 and GX 340+0, with low Q and ν . The other includes Sco X-1 and GX 17+2, which presents relatively high Q and ν .

The detected ν_1 and ν_2 for GX 5-1 range from 156 ± 23 Hz to 627^{+25}_{-13} Hz and from 478 ± 15 to 866 ± 23 Hz, respectively (Jonker et al. 2002). For GX 340+0, ν_1 and ν_2 increase from 197^{+26}_{-70} Hz to 565^{+9}_{-14} Hz and from 535^{+85}_{-48} to 840 ± 21 Hz, respectively (Jonker et al. 2000a,b). These two sources form the lower region in both $Q_1 - \nu_1$ and $Q_2 - \nu_2$ plots. The real maximum may larger than the largest measured value, in fact, the maximum can be at most $\sim 20\%$ higher than the values we used (Mendez 2006), so it seems that the real maxima are too different from the largest values we used in Fig. 2. The same is true for Q_{max} and ν_{max} of other sources. The ν_2 and ν_1 in the other region (including Sco X-1 and GX 17+2) are $\nu_2 \sim 850 - 1150$ Hz and $\nu_1 \sim 500 - 800$ Hz (Homan et al. 2002; van der Klis et al. 1997). In addition, Cyg X-2 covers almost the whole range of Q_2 and ν_2 that the others cover, but a very narrow range for both Q_1 and ν_1 . Because there are just three measurements of Q_1 for this source, it is difficult to infer any implication.

XTE J1701-462 presents the link between "Z-track", " ν -track" and Atoll behavior in its CCD and HID (Homan et al. 2006a,b, 2007; Lin et al. 2009; Homan et al. 2010). Both upper and lower QPOs were detected in Z phase (Sanna et al. 2010). The Z phase of XTE J1701-462 presents quite large errors for both Q_1 and Q_2 , and the frequencies cover the narrow range. The Q_2 are higher than Q_1 for this source, which is different with that of the other Z sources. We think the transition between Atoll and Z state of XTE J1701-462 may link to the accretion rate. When the companion is near

periastron, the neutron star may have higher accretion rate, its magnetosphere will compress and show a higher magnetic field, then the system shows Z state. On the contrary, when the companion is near apastron, the neutron star may have lower accretion rate, the magnetosphere will expand and show a lower magnetic field, then the system shows Atoll state. But it needs more observational and theoretical investigation.

It is noticed that most data points follow an increasing trend in $Q_1 - \nu_1$ diagram (see the right panel of Fig. 2), but an abrupt drop occurs for Sco X-1 at about 750 Hz. Zhang et al. investigated the correlation between upper and lower kHz QPOs in a statistical way (Zhang et al. 2006). They found the power law correlation can fit the data much better than other correlations, e.g. linear relation and constant relation. At the same time, they also found that the power law index shows a turn-over frequency at about $\nu_2 = 840$ Hz in ν_2 vs. ν_1 plot of Z source, which is analogical with the abrupt drop in Q_1 vs. ν_1 plot of Sco X-1. But, we are not sure whether it results from the physical process or from the data itself. If it is a physical reason, it implies that the boundary of the accretion disk and magnetosphere, at where the kHz QPOs are assumed to emit this particular frequency, may occur a physical transition. From the Alfvén wave model for kHz QPOs (Zhang 2004), the disk radius of emitting this particular frequency is about 20 km, or 5 km away from the stellar surface for the star parameters of 15 km and one solar mass (Zhang et al. 2010).

2.3 The $Q - \nu$ Correlations for Atoll Sources

From the left panel of Fig. 3, it is seen that most Q_2 increases with ν_2 steadily, only the source 4U 1728-34 shows an explicit drop at about $\nu_2 \sim 1090.4$ Hz with a maximum of $Q_2 = 14.4 \pm 3$. The Kepler orbital radius corresponding to 1090.4 Hz is about ~ 17 km for a NS of 1.4 solar mass. Thus, the position of turn-over frequency is close to the innermost boundary of the accretion disk and it may reflect the corresponding physical process there. The innermost stable circular orbit (ISCO) of a NS with mass of 1.4 solar mass is ~ 12.6 km, which is the same order as the theoretical radius of NS. We do not know the actual NS mass of 4U 1728-34, so we are not sure whether the ISCO is larger than the star radius. We think that, no matter in which case, the accretion matter may drop because of entering the ISCO boundary or impact onto the surface of the star, and then the system may show an abrupt drop of Q factor. However, the right panel of Fig. 3 presents a very different scenario. Almost all sources display rising, maximum and dropping tendency in the

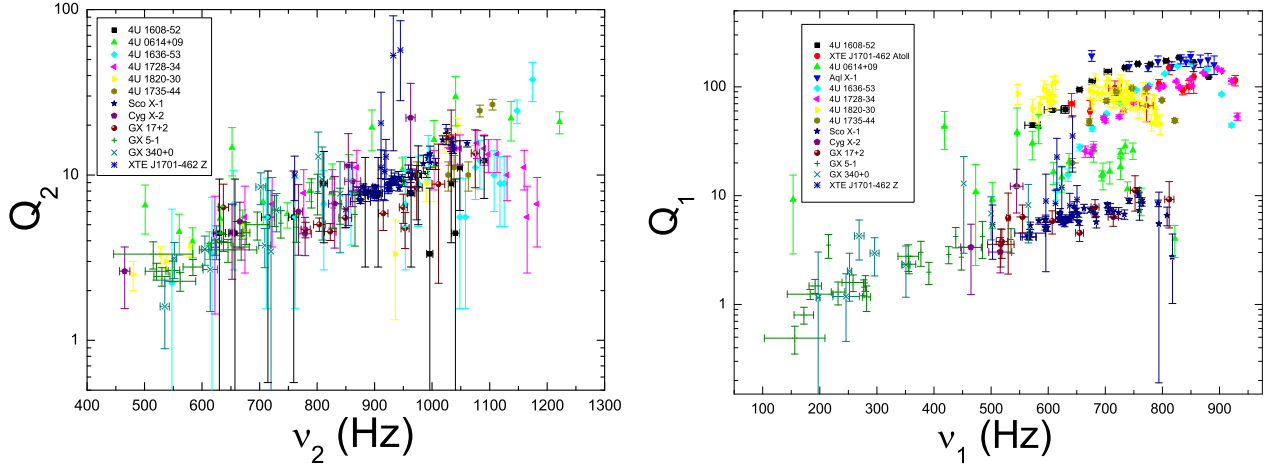


Fig. 1 Plots for $Q - \nu$ relations of kHz QPOs. The left panel is the $Q - \nu$ relations for upper kHz QPOs, and the right one is that for lower kHz QPOs. The meanings of different symbols are listed in the diagrams.

$Q_1 - \nu_1$ diagram. Five sources (4U 1608-52, 4U 1636-53, 4U 1728-34, 4U 1820-30 and 4U 1735-44) present obvious dropping tendency after the maximum Q_1 . The maximums are different for each source. 4U 1608-52, 4U 1636-53, 4U 1728-34 present higher Q_1 (The detected maxima are 247.0 ± 16.0 , 248.0 ± 18.0 , and 188.0 ± 18.0 , respectively) with wider ν_1 ranges. The narrowest ν_1 range of 4U 1735-44 is from 642 to 821 Hz. There is also a gap of ν_1 (between 613 and 673 Hz) in 4U 1820-30. The Q_1 of Aql X-1 are high and cover a very narrow range ($151 \pm 13.2 - 193.8 \pm 22.2$), and so does that of the peak frequency ($696.1 \pm 0.15 - 890.7 \pm 0.37$ Hz). It seems that the kHz QPO frequencies just are detected at the inflexion of $Q_1 - \nu_1$ track. The Q_1 for 4U 0614+09 are relatively low and irregular with large errors, and the maximum is 43.12 ± 16.45 at $\nu_1 = 418.3 \pm 1.8$ Hz. The points which are higher than $Q_1 = 30$ presents very large error bars, and most of the Q_1 are lower than 30. For the Atoll phase of XTE J1701-462, we use the data from the paper by (Sanna et al. 2010) for our plot. It is found that the maximum Q_1 is 150.3 ± 20.9 at 811.5 ± 6.6 Hz, and above this frequency the Q_1 values begin to drop.

3 Discussions

3.1 Relations between $Q - \nu$ Tracks and CCDs Tracks for Z Sources

In spite of some similar respects (Stella 1986), the tracks in CCDs and HIDs for Z sources, by secular timing inspection, can be divided into two types according to qualitative differences (Kuulkers et al. 1994), i.e. Cyg-like sources (Cyg X-2, GX 5-1 and GX 340+0) and

Sco-like sources (Sco X-1 and GX 17+2) (Hasinger et al. 1989; Hasinger 1990). Recently, it is claimed that the Cyg-like sources follow a "Z-track" in CCDs which have a long horizontal branch and form a "Z" profile, while the Sco-like sources present a " ν -track" which have a short horizontal branch and form a " ν " profile (Homan et al. 2007). According to the recent data obtained with PCA on board RXTE, the five typical sources (Cyg X-2, GX 5-1, GX 340+0, Sco X-1 and GX 17+2) can be divided into two subclasses. Cyg X-2, GX 5-1, and GX 340+0 present "Z-track" (Jonker et al. 2000a,b, 2002; Wijnands et al. 1998). Besides, GX 17+2 and Sco X-1 exhibit " ν -track" with not well defined HB/NB vertex, since the HB is almost a continuation of the NB (Homan et al. 2002). The kHz QPOs are detected on the vertex of HB/NB and the upper NB. It is claimed that the properties of kHz QPOs closely related to the position of the sources on the Z track traced out in CCDs, and the frequencies of kHz QPOs increase from the left of HB to NB/FB vertex (Wijnands et al. 1997).

It seems that the division between Sco-like and Cyg-like sources can be in terms of frequency for kHz QPOs. The Cyg-like sources present much longer HB, and it is found that the kHz QPOs in this class of sources are observed at lower frequencies compared with the other two Z sources (Jonker et al. 2000a,b, 2002; Wijnands et al. 1998). In addition, a transition from Cyg-like phase to Sco-like phase occurs in Cyg X-2. This property may be consistent with its wide ν_2 range and the kHz QPOs at relatively high frequencies. However, the Q_1 and ν_1 lie in a very narrow region, but with large error. The physical reason why the other sources don't cover the whole range and Cyg X-2 does will be investigated in our future work. Sco X-1 is a very bright Z source, in

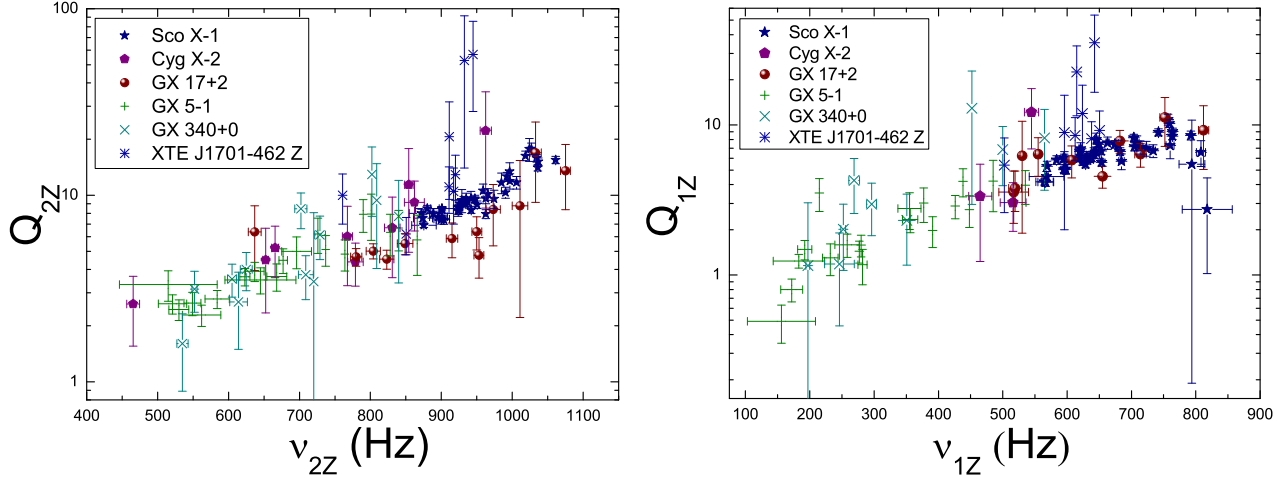


Fig. 2 Plots for $Q - \nu$ relations for Z sources. The left panel is for upper kHz QPOs, and the right one is for lower kHz QPOs. The meaning of different symbols are listed in the diagrams.

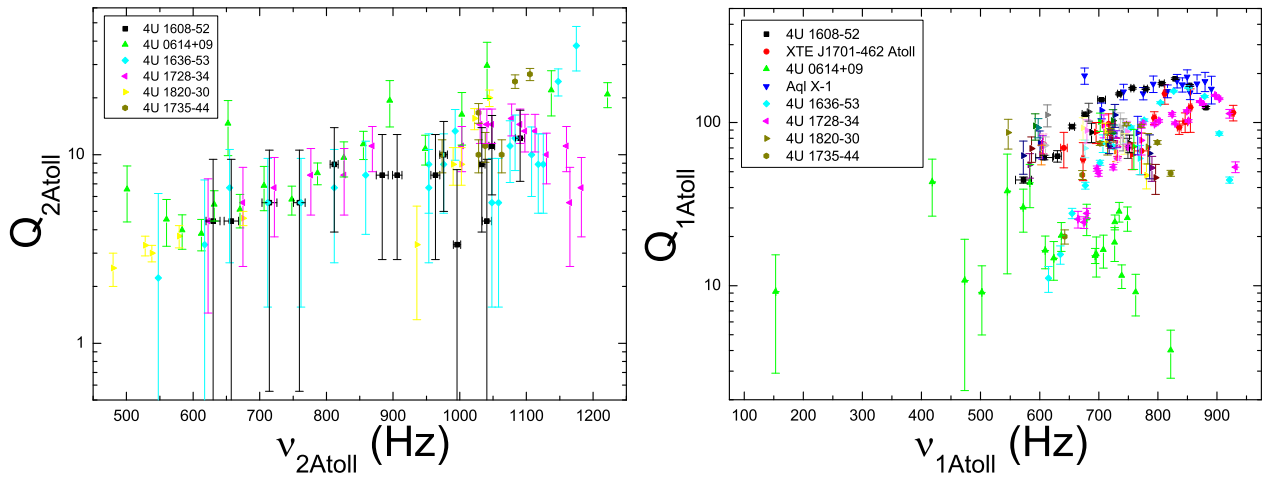


Fig. 3 The same meaning as Fig. 2, but for Atoll sources.

which the kHz QPOs can be detected all the way onto the FB, corresponding to the high frequencies that are observed. Besides, the high luminosity corresponds to the high accretion rate and it may have some possible reasons: One possibility is that the accretion disk is thickened by the radiation pressure during the Z stage. As a result, the magnetosphere of neutron star expands, while both the inner disk radius and the mass accretion rate increase. The signal may be sucked by the thickened disk and the system shows a drop of Q factor. Another possibility is that the innermost boundary of accretion disk is close to the NS surface. Consequently, the radius of magnetosphere is relatively small, and the frequency of kHz QPO can be up to a high value. The region between innermost disk and the NS surface become narrow. So the Q_1 can be up to the relatively high values. When the innermost disk is more close to NS surface, the radiation is sucked by some material accreted by the NS. As a result, the Q_1 begins to drop abruptly with ν_1 .

3.2 The correlation among $Q - \nu$ track, spin frequency and sideband frequency

The peculiar trends of Q_1 as the function of ν for Atoll sources imply the special physics in the inner disk region of these class of sources. The high values of Q_1 indicate the small range of frequency drift for lower kHz QPOs. It is claimed that the drop of Q_1 is a hint of the innermost stable boundary of accretion disk (Miller et al. 1998; Barret et al. 2005c). The maximum of Q_1 is detected at a mildly higher frequency than that of Z sources which is consistent with the small radius of innermost disk. However, the Atoll sources present low luminosity (van der Klis 2006) and low accretion rate. Accordingly, the magnetic field should be mildly weaker than that of Z sources, allowing for the accretion disk extending to be close to the NS surface.

From the second part of section 2, we know that three sources (4U 1608-52, 4U 1636-53 and 4U 1728-34) exhibit very high Q_1 values. Moreover, the spin frequencies have been detected for these sources, i.e. 619Hz (Hartman et al. 2003), 581Hz (Strohmayer et al. 1998; Wijnands et al. 1997; Zhang et al. 1997), 363Hz (Strohmayer et al. 1996c), respectively. In addition, all the three sources display the sideband in their PDS (Jonker et al. 2000a,b). The differences in frequencies between the sidebands and the lower kHz QPOs are, $52.8 \pm 0.9\text{Hz}$ (4U 1608-52), $58.4 \pm 1.9\text{Hz}$ (4U 1636-53) and $64 \pm 2\text{Hz}$ (4U 1728-34) (Jonker et al. 2000a,b). Maybe the high values of Q_1 of the three sources allow for the detection of sidebands, while the sidebands may be engulfed by the boarder peak in other sources.

In order to investigate the relations between spin frequency / sideband frequency and the maximum Q_1 , we fit the function GCAS to the data of these sources and find out the maximum Q_1 for every sources (see Table 1). Then we plot the spin frequency versus Q_{1max} and the difference between sideband frequency and the lower frequency versus Q_{1max} . We also fit an exponential relation to them (see Fig. 4). The fitting results are listed in Table 2 and Table 3. We notice that the source with higher maximum Q_1 present higher spin frequency (see the left panel of Fig. 4), while the difference between ν_1 and the sideband frequency is low (see the right panel of Fig. 4).

The high maximum of Q_1 implies that the emission site of lower kHz QPOs is more close to the NS surface. Besides, the high spin frequency is consistent with a small corotation radius (Zhang 2007). With small corotation radius, the drift range of frequency between this radius and the NS surface is narrow, which corresponds to the high value of Q_1 . Accordingly, this give us the hint that the lower kHz QPOs may relate to the corotation radius. The source with high spin frequency and high maximum value of Q_1 presents the small difference between sideband frequency and ν_1 . So we claim that the emissions of lower kHz QPOs and the sideband are spin mediated.

3.3 Revelation for The Nature of kHz QPOs

The upper frequency is the same order as the dynamical time-scales of the innermost region of the accretion flow around the stellar mass compact objects (van der Klis 2006, 2008). It is considered that ν_2 is the innermost orbital frequency of accretion flow both for Z and Atoll sources. Due to some instabilities resulting from the changes of accretion rate, magnetic pressure and others (Romanova et al. 2007; Rastatter & Schindler 1999; Kulkarni & Romanova 2008), the boundary of inner disk is changing during the accretion process. As a consequence, every peak of kHz QPO signal presents drift around the centroid frequency, contributing to the upper quality factor Q_2 (Wang et al. 2011).

As far as the nature of lower kHz QPOs, two very different evolutionary scenarios of Q_1 as the function of ν_1 (see the right panels of Fig. 2 and Fig. 3 for a detail) imply distinct physics in the inner disk for Z and Atoll sources. High accretion rate leads to strong instabilities which are responsible for the large frequency drift. So the values of Q_1 for Z sources are low. For the Atoll sources, the accretion flow with low accretion rate and the relatively stable scenario in the inner region of disk allows for the disk extending all the way to near the NS surface, which accounts for the high values of Q_1 .

Table 1 The fitting results for Q_{1max} of three Atoll sources.

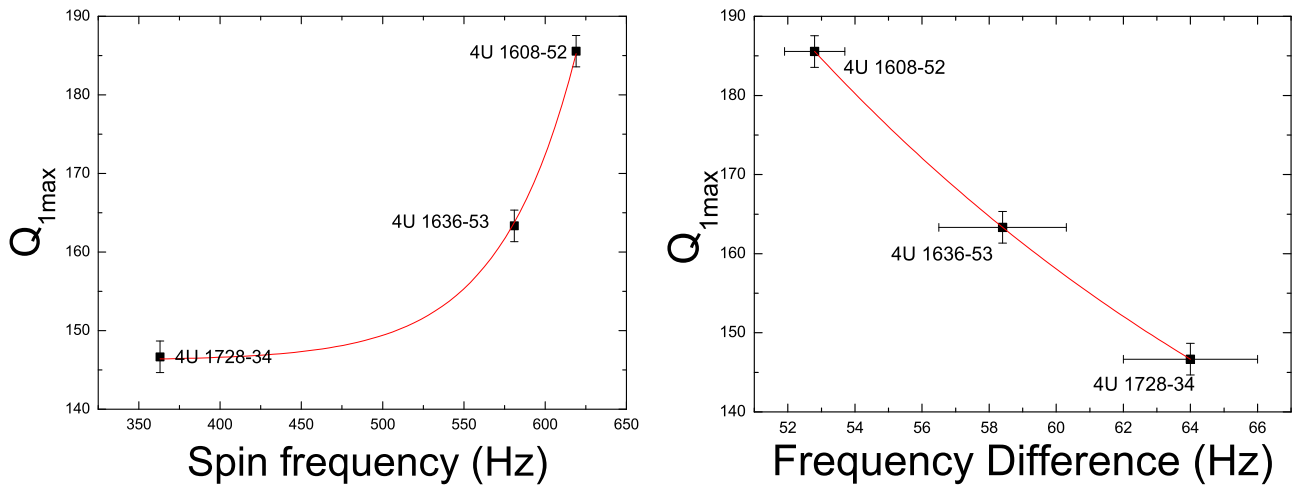
| Source | Q_{1max} | error(Q) | ν_1 | error(ν_1) |
|------------|------------|----------|---------|------------------|
| 4U 1608-52 | 182.9 | 3.2 | 824.03 | 3.02 |
| 4U 1636-53 | 168.15 | 4.2 | 833.9 | 2.28 |
| 4U 1728-34 | 143.61 | 2.9 | 872.57 | 3.2 |

Table 2 The fitting results for spin frequency versus Q_{1max} .

| Relation | a | b | c | d |
|--------------------|--------|---------|--------|--------|
| $y = a^{bx-c} + d$ | 1.0216 | 0.98602 | 438.85 | 146.22 |

Table 3 The fitting results for the difference between ν_1 and sideband frequency versus Q_{1max} .

| Relation | a | b | c | d |
|--------------------|---------|---------|----------|---------|
| $y = a^{bx-c} + d$ | 0.89119 | 0.44606 | 62.50412 | 96.6845 |

**Fig. 4** The fittings for the correlations between spin frequency / frequency difference and Q_{1max} . The left panel is for the spin frequency versus Q_{1max} . The right one is for the difference between ν_1 and sideband frequency versus Q_{1max} .

We expect to find out the hints for mechanism of lower kHz QPOs from the nature of Z and Atoll sources in our future work.

4 Summary

More and more data about the coherence of kHz QPOs in NS LMXBs are detected, the $Q - \nu$ relations and their implications have been the attractive issues. In this paper, we investigate the recently published data of quality factors for thirteen sources (Mendez 2006; Sanna et al. 2010), i.e. seven Atoll sources (4U 1608-52, 4U 1636-53, 4U 1728-34, 4U 0614+09, Aql X-1, 4U 1820-30 and 4U 1735-44), five Z sources (Sco X-1, Cyg X-2, GX 17+2, GX 5-1 and GX 340+0) and XTE 1701-462 which presents both Z and Atoll behaviors. The main conclusions are listed below.

(1). The Q_2 values are low ($Q_2 \sim 2 - 20$) for both Z and Atoll sources. The $Q_2 - \nu_2$ tracks increase steadily, in general. The values of Q_1 are low ($Q_1 \sim 2 - 20$) for Z sources and increase with frequencies (except for Sco X-1). But the values of Q_1 for Atoll sources are very high (up to 200), and increases with frequencies up to a maximum then abruptly drops.

(2). Though the $Q - \nu$ distribution of Z sources form a continues relation for both upper and lower kHz QPOs, they can be divided into two regions, according to the ranges of ν . One contains Sco X-1 and GX 17+2, which present high Q -values and high centroid frequencies. The other is formed by GX 5-1 and GX 340+0, with low Q -values and centroid frequencies. However, Cyg X-2 extends almost to the whole range of Q_2 and ν_2 that the others cover. The different ranges of frequency may give us useful information about the nature of Z and Atoll source.

(3). The ν_2 for Atoll sources cover a boarder range and Q_2 values are low 2 – 20. Almost all $Q_1 - \nu_1$ tracks for Atoll sources present rising part, maximum and then the abrupt drop.

(4). The spin period and sidebands were detected in three sources (4U 1608-52, 4U 1636-53 and 4U 1728-34) which present very high Q_1 . The source with higher spin frequency presents higher Q_1 values, and its difference between lower ν_1 and sideband frequency is low.

(5). The Q_1 values are the same order as Q_2 for 4U 0614+09. The lower frequencies for Aql X-1 just were detected in a very narrow range, and the Q_1 values are high. XTE 1701-462 presents high errors for Q_2 and Q_1 .

(6). The emission of lower kHz QPOs and sideband frequency may be correlated to the NS spin.

Acknowledgements We acknowledge M. Mendez and D. Barret for providing the data. It is also a pleasure to thank M. A. Abramowicz, G. Q. Ding, J. Horák and W. Kluźniak for helpful discussions. This work is supported by National Basic Research Program of China (2009CB824800, 2012CB821800), the National Natural Science Foundation of China (NSFC 10773017, NSFC 10773034, NSFC 10778716, NSFC 11173024), NSC 99-2112-M-007-017-MY3 and the Fundamental Research Funds for the Central Universities.

References

- Barret, D., Boutelier, M., & Miller, M. C.: MNRAS **384**, 1519 (2008)
- Barret, D., Kluźniak, W., Olive, J. F., Paltani, S., Skinner, G. K.: MNRAS **357**, 1288 (2005a)
- Barret, D., Olive, J. F., Miller, M. C.: MNRAS **361**, 855 (2005b)
- Barret, D., Olive, J. F., Miller, M. C.: Astron. Nachr. **326**, 808 (2005c)
- Barret, D., Olive, J. F., Miller, M. C.: MNRAS **370**, 1140 (2006)
- Barret, D., Olive, J.-F., & Miller, M. C.: MNRAS **376**, 1139 (2007)
- Boutelier, M., Barret, D., & Miller, M. C.: MNRAS **399**, 1901 (2009)
- Boutelier, M., Barret, D., Lin, Y., Török, G.: MNRAS **401**, 1290 (2010)
- Campana S.: ApJ **534**, L79 (2000)
- Gladstone, J., Done, C., Gierlinski, M.: MNRAS **378**, 13 (2007)
- Hartman, J. M., Chakrabarty, D., Galloway, D. K., Muno, M. P., Savov, P., Mendez, M., van Straaten, S., Di Salvo, T.: in HEAD meeting 7, Bulletin of the American Astronomical Society, Vol. 35, p.865 (2003)
- Hasinger, G.: RvMA **3**, 60 (1990)
- Hasinger, G., & van der Klis, M.: A&A **225**, 79 (1989)
- Homan, J. et al.: ApJ **656**, 420 (2007)
- Homan, J. et al.: ApJ **719**, 201 (2010)
- Homan, J., Belloni, T., van der Klis, M., Casella, P., Mendez, M., Lewin, W., Fender, R., Gallo, E., & Gehrels, N.: Astron. Tel. **725**, 1 (2006a)
- Homan, J., Belloni, T., van der Klis, M., Casella, P., Mendez, M., Lewin, W., Fender, R., Gallo, E., & Gehrels, N.: Astron. Tel. **748**, 1 (2006b)
- Homan J., van der Klis M., Jonker P. G., Wijnands R., Kuulkers Erik; Méndez M., Lewin W. H. G.: ApJ **568**, 878 (2002)
- Jonker, P. G. et al.: ApJ **537**, 374 (2000)
- Jonker, P. G., Méndez, M. & van der Klis, M.: astro-ph/0008358 (2000)
- Jonker, P. G., van der Klis, M., Homan, J., Méndez, M., Lewin, W. H. G., Wijnands, R. & Zhang, W.: MNRAS **333**, 665 (2002)
- Kulkarni, A. K. & Romanova, M. M.: MNRAS **386**, 673 (2008)
- Kuulkers, et al.: A&A **311**, 197 (1994)
- Lin, D. C., Remillard, R. A. & Homan, J.: ApJ **696**, 1257 (2009)
- Méndez, M.: MNRAS **371**, 1925 (2006)
- Miller, M. C., Lamb, F. K., Psaltis, D.: ApJ **508**, 791 (1998)
- Rastätter, L. & Schindler, K.: ApJ **524**, 361 (1999)
- Remillard, R. A. & Lin, D.: Astron. Tel. **696**, 1 (2006)
- Romanova, M. M., Kulkarni, A. K. & Lovelace, R. V. E.: (astroph/ 0711.0418) (2007)
- Sanna, A., Méndez, M., Altamirano, D., Homan, J., Casella, P., Belloni, T., Lin, D. C., van der Klis, M., Wijnands, R.: MNRAS **408**, 622 (2010)
- Stella L.: "Plasma Penetration into Magnetospheres", Iraklion: Cr ete University Press, P.199 (1986)
- Strohmayer, T., Smale, A., Day, C., Swank, J., Titarchuk, L., Lee, U.: IAU Circ., No. 6387 (1996b)
- Strohmayer, T., Zhang, W., Swank, J.: IAU Circ., No. 6320 (1996a)
- Strohmayer, T., Zhang, W., Swank, J., Smale, A., Titarchuk, L., Day, C.: ApJ Lett **469**, L9 (1996c)
- Strohmayer, T. E., Zhang, W., Swank, J. H., White, N. E., Lapidus, I.: ApJ **498**, L135 (1998)
- Török, G.: A&A **497**, 661 (2009)
- van der Klis, M.: ARA&A **38**, 717 (2000)
- van der Klis, M.: A review of rapid X-ray variability in X-ray binaries inn Compact stellar X-ray sources, W.H.G. Lewin & M. van der Klis (eds.), Cambridge University Press, p. 39; (astro-ph/0410551). (2006)
- van der Klis, M.: AIPC. **1068**, 163 (2008)
- van der Klis, M., Swank, J., Zhang, W., Jahoda, K., Morgan, E. et al.: IAU Circ. No. 6319 (1996a)
- van der Klis, M., Swank, J., Zhang, W., Jahoda, K., Morgan, E. et al.: ApJ Lett **469**, L1 (1996b)
- van der Klis M., Wijnands R.: ApJ **481**, L97 (1997)
- van der Klis, M., Wijnands, R., Chen, W., Lamb, F. K., Psaltis, D. et al.: IAU Circ. No. 6424 (1996c)
- Wang, J., Zhang, C. M., Zhao, Y. H., Lin, Y. F., Yin, H. X., and Song, L. M.: A&A **528**, 126 (2011)
- Wijnands, R. A. D., van der Klis, M., van Paradijs, J., Lewin, W. H. G., Lamb, F. K., Vaughan, B., Kuulkers, E.: ApJ Lett **479**, L141 (1997)
- Wijnands, R., Homan, J., van der Klis, M., Kuulkers, E., van Paradijs, J., Lewin, W. H. G., Lamb, F. K., Vaughan, B.: ApJ **493**, L87 (1998)
- Zhang C. M.: A&A, 423, **401** (2004)
- Zhang C. M., Yin H. X., Zhao Y. H., Zhang F. & Song L. M.: MNRAS, **366**, 1373 (2006)
- Zhang, C. M.: AdSpR **40**, 1480 (2007)
- Zhang C. M., Wei Y.C. & Yin H.X. et al.: Science in China (G), **53**, 114 (2010)
- Zhang, W., Lapidus, I., Swank, J. H., White, N. E., Titarchuk, L.: IAU Circ. **6541**, 1 (1997)